Polyhedron 155 (2018) 281–290

Contents lists available at ScienceDirect

Polyhedron

journal homepage: www.elsevier.com/locate/poly

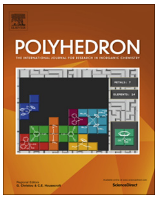

Tuning iridium (I) $PC_{carbene}P$ frameworks for facile cooperative N_2O reduction

Joel D. Smith [a], Edwina Chih [a], Warren E. Piers [a,*], Denis M. Spasyuk [a,b]

[a] *Department of Chemistry, University of Calgary, 2500 University Drive NW, Calgary, Alberta T2N 1N4, Canada*
[b] *Canadian Light Source Inc., 44 Innovation Boulevard, Saskatoon, Saskatchewan S7N 2V3, Canada*

ARTICLE INFO

Article history:
Received 10 July 2018
Accepted 17 August 2018
Available online 30 August 2018

Dedicated to Prof. Bill Jones, a giant of organometallic chemistry, on the occasion of his 65th birthday.

Keywords:
PCP Pincer Ligands
Iridium
Nitrous oxide reduction
Ligand design
Metal–ligand cooperativity

ABSTRACT

Two electron-rich PCP ligands were synthesized featuring $–C(CH_3)_2–$ and $–Si(CH_3)_2–$ functional groups linking the framework backbone. $PC_{carbene}P$–Ir–Cl complexes were prepared *via* double C–H activation protocols and the donor strengths of the new ligands were evaluated using CO stretching frequencies of monocarbonyl cations prepared from the corresponding carbene chlorides. The new tethered systems were found to be superior donors with respect to $PC_{carbene}P$ pincer complexes previously reported in our group. These carbene chloride complexes reacted readily with nitrous oxide (N_2O) to form "iridaepoxides" immune to unwanted $C_{aryl}–C_{anchor}$ cleavage. Rates of oxygen atom transfer from N_2O to a series of $PC_{carbene}P$–Ir–Cl compounds were also measured using $^{31}P\{^1H\}$ NMR spectroscopy. Results suggested a direct positive correlation between ligand donicity and O-atom transfer rate for all *ortho*-phenylene derived systems. The sterically distinct 2,3-benzo[*b*]thiophene scaffold was found to be an outlier of this trend with a relatively high reactivity rate and ν_{CO}.

1. Introduction

Since the seminal work of Moulton and Shaw [1], metal complexes supported by pincer ligands have become important fixtures in homogeneous catalysis [2]. Participating in a large array of chemical reactivity, from alkane dehydrogenation [3] to CO_2 reduction [4], pincer complexes have shown great versatility due to easily modifiable, rigid scaffolds that exhibit great thermal stability [2,5]. Tridentate pincer ligands consist of three two-electron donor atoms – typically, but certainly not limited to, phosphorus, nitrogen and carbon – chelated in a coplanar fashion around a metal centre [2,6]. The coordinated atoms may be present in a variety of combinations and ligands are categorized by the flanking and central atoms using elemental symbols for their designation (i.e. PNP, PCP, etc.; Scheme 1) [7].

While conventional organometallic reactions take place at the metal centre, several transformations have been observed with a ligand directly participating along with the metal; this is known as metal–ligand cooperativity (MLC) [8,9]. Pincer complexes are no exception and in recent years research has indicated MLC can play a tremendous role in promoting the activation of small molecules, such as H_2, NH_3, CO_2 and H_2O [8,10,11]. More recently, there has been interest in the activation and catalytic reduction of nitrous oxide (N_2O), a relatively inert and potent greenhouse gas [12,13]. Early studies utilized the ability of N_2O to insert an oxygen atom into M–H bonds as a means of substrate activation, with subsequent reductive elimination of H_2O to complete the hydrogenation cycle [14–16]. Gianetti and co-workers similarly propose "conventional" N_2O activation in reactions that utilize nitrous oxide as a hydrogen acceptor or oxygen atom transfer agent [17,18]. In contrast, Milstein and co-workers have demonstrated the catalytic hydrogenation and hydrosilation of N_2O proceeds *via* a MLC mechanism involving ligand aromatization/dearomatization using a ruthenium PNP complex [19].

In this context, we found that iridium $PC_{carbene}P$ pincer complexes interact with N_2O *via* a distinct type of MLC. The Ir═C linkages anchoring these pincer ligands are more "Fischer-like" [20–22] and quite capably form "iridaepoxides" through the addition of an oxygen atom across an M═C bond when exposed to N_2O (**B**, Scheme 2) [23]. These iridaepoxides add hydrogen to give a dihydride species **C**, [23,24] but this thermodynamic isomer must convert to a kinetic species where the hydride ligands are *cis* to the O atom in order to release H_2O. While H_2O could be released with heating, catalytic turnover in these systems was hampered by the high barrier to water elimination from **C** and unfavorable relative kinetics of N_2O vs H_2 addition to the Ir═C bond. Furthermore, in the presence of H_2 iridaepoxides can undergo unwanted

---

[*] Corresponding author.
E-mail address: wpiers@ucalgary.ca (W.E. Piers).

https://doi.org/10.1016/j.poly.2018.08.054
0277-5387/© 2018 Elsevier Ltd. All rights reserved.

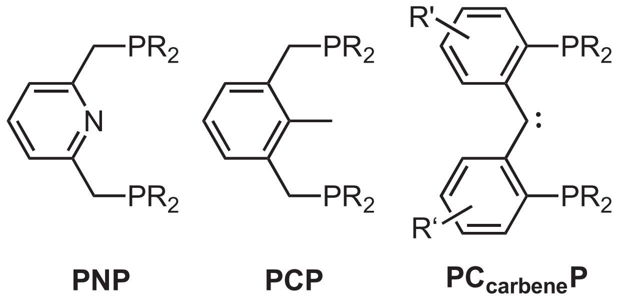

Scheme 1.

C_{aryl}–$C_{cleavage}$ [25]. Since many of these problems stemmed from slow N_2O reactions with the Ir═C species **A**, we sought ways in which to increase the rate of this reaction relative to H_2 addition through ligand design. We hypothesized that more electron donating, and rigid ligand frameworks would facilitate this reaction, while slowing the addition of H_2 to the Ir═C bond to give coordinatively saturated Ir(III) hydrido chloride species [22].

Recently our group ranked a series of iridium $PC_{carbene}P$ complexes (**1** to **4-Cl**, Scheme 3) according to ligand donor strength by preparing cationic carbonyl and dicarbonyl derivatives and cataloguing the CO stretching frequencies [26]. Among this collection was the tethered system **4-Cl**, which exhibited an intermediate ligand donor strength relative to **2-Cl** and **3-Cl**. However, preliminary experiments showed that the more rigid ligand framework in **4-Cl** rendered it immune to C_{aryl}–C_{anchor} cleavage and furthermore that it reacted much more rapidly with N_2O than **2-Cl** (but slower than the more electron rich **3-Cl**). It thus appeared as though ligand donor ability could be exploited to enhance reactivity at the M═C bond, while rigid ligands prevent C–C bond cleavage deactivation pathways. Therefore, we designed similarly rigidified but more electron-rich derivatives. Herein, we report the synthesis and characterization of the two new iridium $PC_{carbene}P$ complexes, **5-Cl** and **6-Cl**. Mono- and dicarbonyl cationic derivatives are prepared and carbonyl stretching frequencies (ν_{CO}) are used to gauge ligand donicity. Reaction profiles of complexes **1** through **6-Cl** with N_2O are compared alongside their ν_{CO} to reveal any trends linking donor strength and reaction rate.

2. Results and discussion

Previously, we established a method for preparing an electron rich, rigidified iridium $PC_{carbene}P$ system **4-Cl** [26]. However, the cumbersome 14 step synthesis from 1,3,5-tribromobenzene and unexpectedly low ligand donor strength relative to **3-Cl** suggested that replacing the electronegative O linker in the ligand of **4-Cl** with a more electron donating fragment like –C(CH_3)$_2$– or –Si

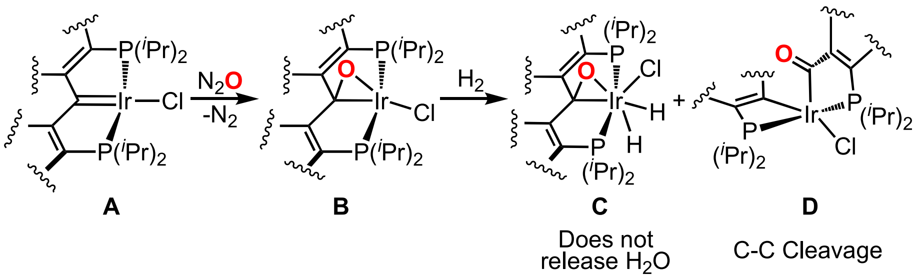

Scheme 2.

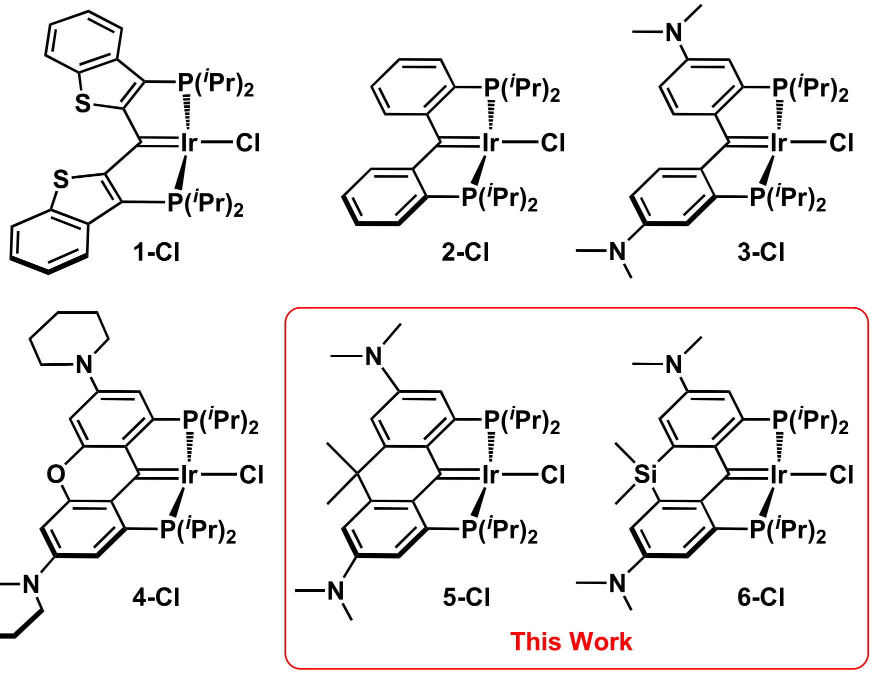

Scheme 3.

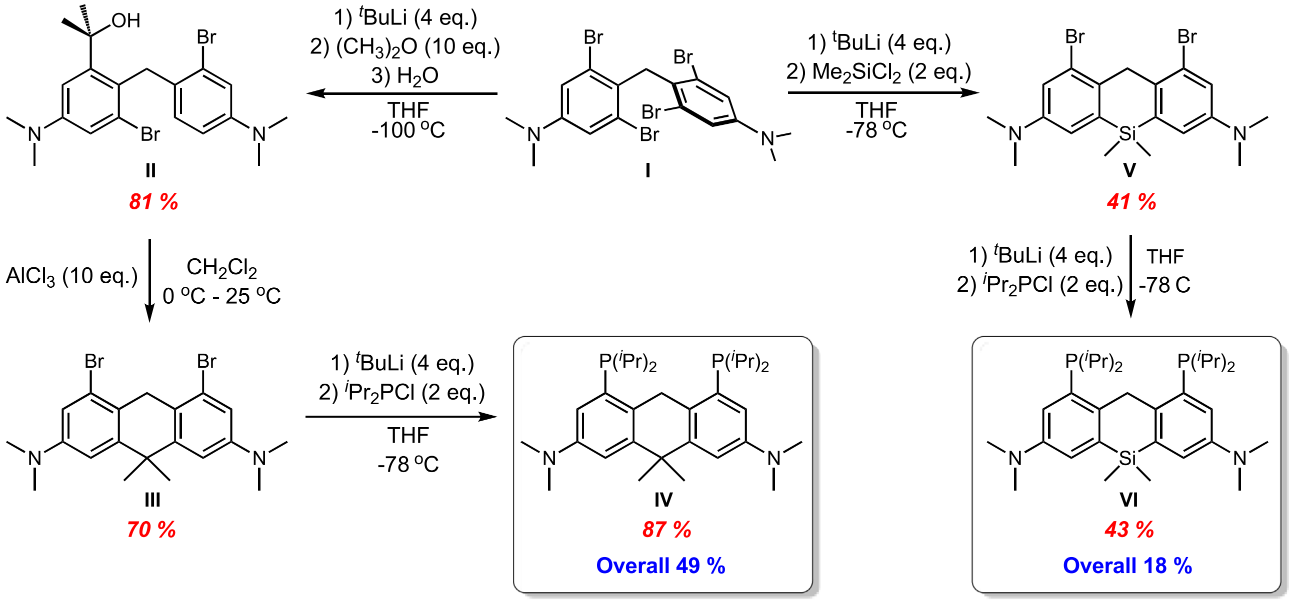

Scheme 4.

$(CH_3)_2$– would both increase the donor properties of the ligand framework and lower the synthetic pain necessary to obtain workable quantities of ligand. As shown in Scheme 4, both ligands **IV** and **VI** can be obtained from the common intermediate **I**, which was prepared in multigram quantities in two steps starting with 3,5-dibromo-aniline via modified literature procedures [27,28] (see the Supporting Information for further details on the synthesis of **I**). Compound **I** could be selectively lithiated once on each aryl ring in THF at −100 °C using *tert*-butyllithium and then quenched with either acetone (to form **II**) or dimethyldichlorosilane (to give **V**). For **II**, an excess of dry acetone was added to *in situ* generated dilithio reagent to ensure complete conversion of material in a timely fashion; extended reaction times or warming resulted in the formation of unwanted side products, as observed by GC–MS. Fortunately, the addition of one bulky hydroxyl isopropyl group was enough to prevent the addition of a second despite the use of excess acetone. Compound **II** was therefore furnished cleanly and in good yield after quenching the reaction mixture with water and workup. Using methodology employed on a closely related substrate [29], 4,5-dibromo-N^2,N^2,N^7,N^7,9,9-hexamethyl-9,10-dihydroanthracene-2,7-diamine (**III**) was obtained through an intramolecular electrophilic aromatic substitution of **II** using an excess of $AlCl_3$; the air sensitivity of this compound was immediately noted as the isolated pale yellow solid changed to a dark blue-green colour after exposure to ambient atmosphere. Compound **III** was then lithiated under inert atmosphere with *tert*-butyllithium and the dilithio species quenched *in situ* using two equivalents of chlorodiisopropylphosphine as the electrophile. This sequence gave pincer proligand **IV** as a pale yellow solid with an overall 49% yield in 3 steps from **I**. The ligand **VI**, incorporating the more electropositive –$Si(CH_3)_2$– linker also prepared from the dilithio reagent obtained from **I** by quenching with Me_2SiCl_2 to afford **V**. After work-up of **V** the isolated solid was again lithiated and the phosphino-groups were installed using chlorodiisopropylphosphine to give the silated proligand **VI** in an overall yield of 18% over 2 steps from **I**.

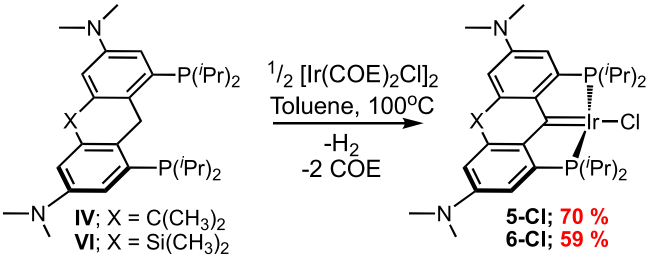

Scheme 5.

With these new proligands in hand, well established double C–H activation procedures [22,30] were employed to prepare the iridium $PC_{carbene}P$ complexes **5-Cl** and **6-Cl** directly from the proligands **IV** and **VI** and $[Ir(COE)_2Cl]_2$ as an iridium source (Scheme 5). The –$C(CH_3)_2$– linked carbene **5-Cl** was easily synthesized at 100 °C in toluene in a sealed thick-walled glass pressure reaction vessel. Unlike **5-Cl** the silated compound **6-Cl** was prepared in an open system under a blanket of argon to help with removal of any formed H_2 gas that could produce unwanted Ir (III) hydrido-chloride species similar to those observed with the parent system **2-Cl** [22]. Both **5-Cl** and **6-Cl** were isolated with moderate yields of 70% and 59%, respectively, and ^{13}C {^1H} NMR revealed the characteristic carbene triplets at 194.2 ppm ($^2J_{CP}$ = 2.9 Hz) and 200.7 ppm ($^2J_{CP}$ = 2.6 Hz), respectively. The ^{31}P {^1H} NMR signal for **5-Cl** was found at 54.1 ppm, while the signal for **6-Cl** was 47.9 ppm; these shifts are within the typical range observed for this class of compounds [25,26]. Crystallographic data for both compounds were obtained through X-ray diffraction analysis on single crystals; structures are presented in Fig. 1 along with selected metrical data. While two molecules of **5-Cl** were present in the asymmetric unit data for only one is presented as the bond distances and angles between the metal centers and directly associated atoms were quite similar with only minor variations between complexes. Predictably, the bond distances between the aryl rings and the backbone tethers (–$C(CH_3)_2$– and –$Si(CH_3)_2$–) are significantly different with the C7–Si1 and C8–Si1 bond lengths of **6-Cl** being ca. 0.3 Å longer than the C7–C8 and C8–C9 bond lengths in **5-Cl**. Variation in the angle between the aryl rings and the tether is also significant with **5-Cl** having a C7–C8–C9 angle of 113.2(4) Å and **6-Cl** having a C7–Si1–C8 angle of 102.94(11). Despite these differences, the incorporation of the Si atom did not translate to a change in the P–Ir–P angle and Ir–P distances. Therefore, to accommodate this larger atom a more "ruffled" ligand

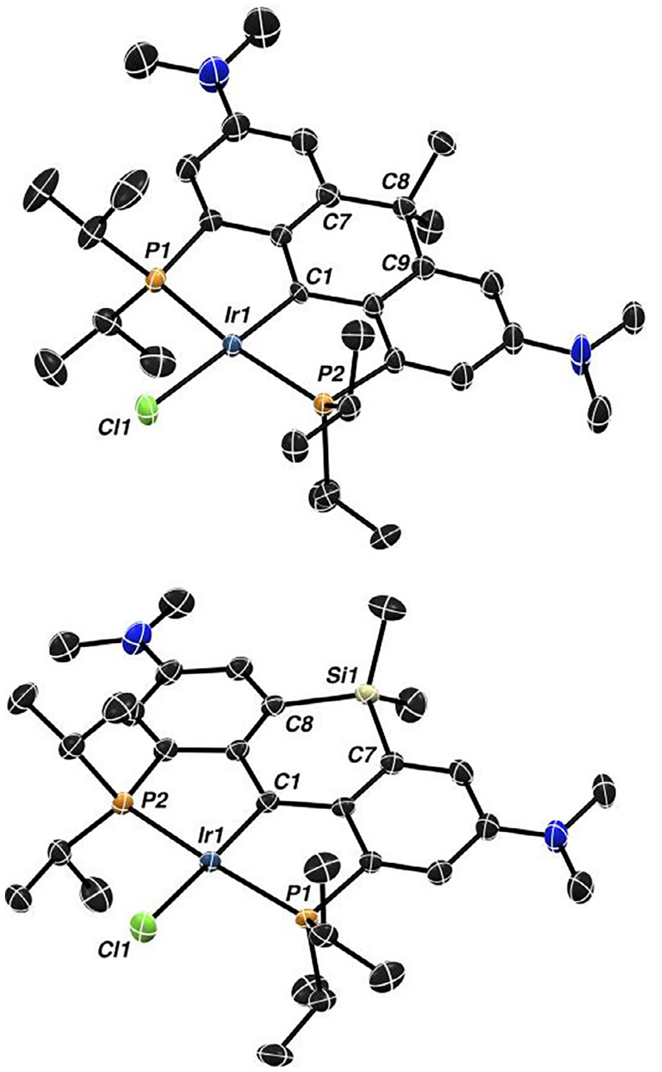

Fig. 1. Thermal ellipsoid diagrams of carbene chlorides **5-Cl** (top) and **6-Cl** (bottom) with thermal ellipsoids drawn to 50% probability. Hydrogen atoms have been omitted for clarity. Selected metrical data for **5-Cl**: Bond distances (Å): Ir1–C1, 1.928(4); Ir1–P1, 2.2654(10); Ir1–P2, 2.2650(10); Ir1–Cl1, 2.4073(11); C7–C8, 1.541(6); C8–C9, 1.534(6). Bond angles (°): P1–Ir1–P2, 167.72(4); C1–Ir1–Cl1, 178.74; C7–C8–C9, 113.2(4). Selected metrical data for **6-Cl**: Bond distances (Å): Ir–C1, 1.936(2); Ir1–P1, 2.2613(6); Ir1–P2, 2.2610(3); Ir1–Cl1, 2.4106(6); C7–Si1, 1.861(3); C8–Si1, 1.860(3). Bond Angles (°): P1–Ir1–P2, 168.58(2); C1–Ir1–Cl, 171.88(7); C7–Si1–C8, 102.94(11).

shape was taken on in **6-Cl** with the aryl rings twisting slightly out of plane resulting in a dihedral angle of 16.1(1)° between the planes defined by the six carbons of the flanking aromatic rings. In comparison, the carbon linked ligand framework remained relatively planar, with the analogous planes defined by the aryl rings having a dihedral angle of only 0.8°(1) and 6.4(3)° for the two molecules in the asymmetric unit cell.

The compounds **3-Cl** [26] and **5-Cl** differ only by the presence or absence of the 2-propyl bridge and a comparison of their structural and spectroscopic properties indicate very few differences. The Ir=C bond lengths were not significantly different with the **3-Cl** bond being 1.902(6) Å. The one major structural difference between the two complexes was the dihedral angles formed by the planes defined by the carbon atoms in each of the aromatic rings. Due to the steric repulsion of the protons *ortho*- to the carbene carbon the aryl rings "ruffled" and the dihedral angle that formed was 44.3(3)°, much larger than that formed in **5-Cl**, *vida supra*. The $^{13}C\{^1H\}$ NMR for **3-Cl** indicated a characteristic triplet at 204.0 ppm ($^2J_{CP}$ = 3.2 Hz; Ir=C) which is only 10.2 ppm downfield from that observed for **5-Cl**. Resonances in the $^{31}P\{^1H\}$ NMR again only slightly differ with **3-Cl** being found upfield by 5.5 ppm at 48.6 ppm. UV–Vis spectra of these two compounds also showed similar profiles (Fig. S19 and S20 in supplemental information); compound **3-Cl** exhibited absorbance maxima (λ_{max}) 600 nm and 795 nm while **5-Cl** showed λ_{max} values of 581 nm and 794 nm.

To place these new ligands onto the scale of donicity previously established for ligands of this type [26], iridium monocarbonyl cationic complexes **5-CO** and **6-CO** (Scheme 6) were prepared by abstracting the chloride ligands using sodium tetrakis[3,5-bis(trifluoromethyl)phenyl]borate ($NaB(Ar^F)_4$) following exposure to carbon monoxide (CO) [26]. Although attempts were made to control the amount of CO added to both **5-Cl** and **6-Cl** we found that adding 1 equivalent of CO followed by chloride abstraction with $NaB(Ar^F)_4$ produced a mixture of both mono-(**5-CO** and **6-CO**) and dicarbonyl compounds (**5-(CO)$_2$** and **6-(CO)$_2$** in Scheme 6) as well as several unwanted side products. Eventually we determined that minimal exposure (ca. 1 s) of **5-Cl** and **6-Cl** to 1 atm. of CO followed by the addition $NaB(Ar^F)_4$ furnished **5-CO** and **6-CO** with less than 10% of the dicarbonyl compounds **5-(CO)$_2$** and **6-(CO)$_2$**. Pure monocarbonyl complexes were then able to be achieved through repeated solvent removal and careful heating of the residue under dynamic vacuum. These compounds were fully characterized spectroscopically and selected data is presented in Table 1 along with previously reported data for compounds **1**–**4-CO** for comparison. (**5-CO** was also characterized crystallographically, see Supplementary Data). The infrared spectra immediately confirmed our hypothesis on ligand design; compounds **5-CO** and **6-CO** were found to have high ligand donor strengths with CO stretching frequencies (ν_{CO}) being 1965 cm^{-1} and 1961 cm^{-1}, respectively, very similar to that for the less stable unlinked system **3-CO**. Dicarbonyl cationic complexes, **5-(CO)$_2$** and **6-(CO)$_2$**, were also prepared by the addition of 1 atmosphere of CO to both monocarbonyl complexes. The symmetric and asymmetric frequencies for the dicarbonyl compounds (Table 1) were quite similar to the other amino functionalized carbenes, **3-(CO)$_2$** and **4-(CO)$_2$**. NMR spectroscopy for these cationic carbenes again showed trends similar to those

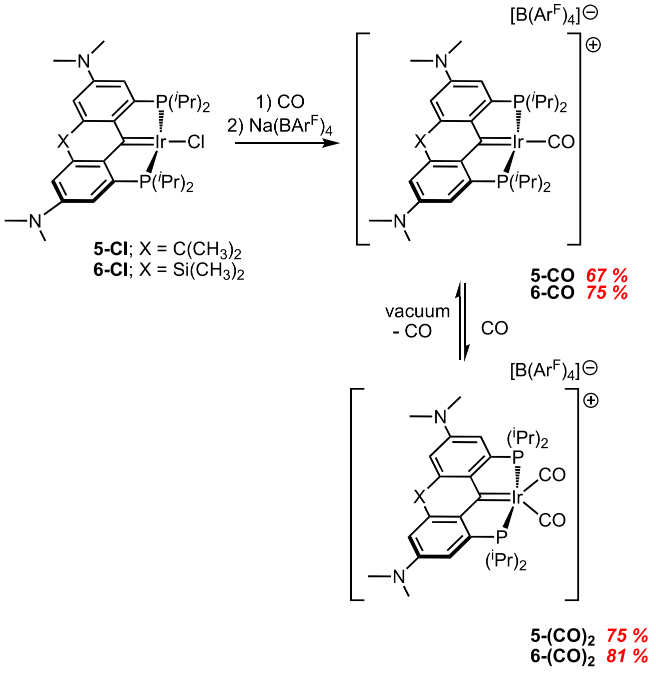

Scheme 6.

Table 1
Compiled spectroscopic data for mono and dicarbonyl cations [26].

Compound	^{31}P (ppm)	$^{13}C_{Ir=C}$ (ppm)	$^{13}C_{CO}$ (ppm)	ν_{CO} (cm^{-1})
1-CO	59.6	232.2	188.6	2048
2-CO	68.6	267.8	195.1	2004
3-CO	72.2	260.4	195.9	1963
4-CO	78.6	214.9	196.4	1974
5-CO	71.8	234.8	195.6	1965
6-CO	68.4	250.5	193.7	1961
1-(CO)$_2$	47.1	200.1	182.1	2055, 2014
2-(CO)$_2$	61.0	233.9	178.2	2050, 2002
3-(CO)$_2$	58.2	242.4	179.7	2014, 1971
4-(CO)$_2$	62.9	207.4	178.2	2014, 1973
5-(CO)$_2$	58.8	226.1	179.1	2014, 1974
6-(CO)$_2$	55.0	240.6	180.4	2018, 1971

synthesized previously with ^{31}P, $^{13}C_{Ir=C}$ and $^{13}C_{CO}$ chemical signals shifting more downfield upon the removal of carbonyl ligand from a dicarbonyl complex.

N_2O was reacted with compounds **2-Cl**, **4-Cl**, **5-Cl** and **6-Cl** to prepare the corresponding previously unreported iridaepoxides **2-Epox**, **4-Epox**, **5-Epox** and **6-Epox** (Scheme 7). This confirmed that these carbene complexes react analogously to what we had previously observed [23,25]. Spectroscopically, all of the reactions were very clean and isolated yields for these complexes were moderate to high. $^{31}P\{^1H\}$ NMR spectroscopy revealed signals within a typical range of 27 ppm to 30 ppm. $^{13}C\{^1H\}$ resonances for the central Ir–C atoms were similarly found in a characteristic range of 72 ppm and 84 ppm. Gratifyingly, the linked compounds **4**–**6-Epox** were not susceptible to C_{aryl}–C_{anchor} cleavage after being exposed to elevated temperatures (>70 °C) and H_2 gas. This stability was further evidenced through examination of the molecular structures of **4-Epox** and **5-Epox**, which were determined using X-ray diffraction of single crystals; thermal ellipsoid diagrams and selected metrical parameters can be found in Fig. 2. Directly comparing the two complexes, the bond lengths and angles between atoms directly associated with the metal centre varied little. The backbone linker bond lengths and angles differed based on the particular linking atom; the C–O–C angle, 117.1(4)°, for **4-Epox** was slightly larger than the C–C–C angle, 112.8(5)°, for **5-Epox**. Notably the central C1 atoms for the complexes appear to have less torsional strain than **3-Epox**. The planes defined by the flanking aryl rings form dihedral angles of 9.8(3)° and 17.8(3)° for **4-Epox** and **5-Epox**, respectively, which, because of the linking atoms, results in a slightly puckered ligand shape. On the other hand a

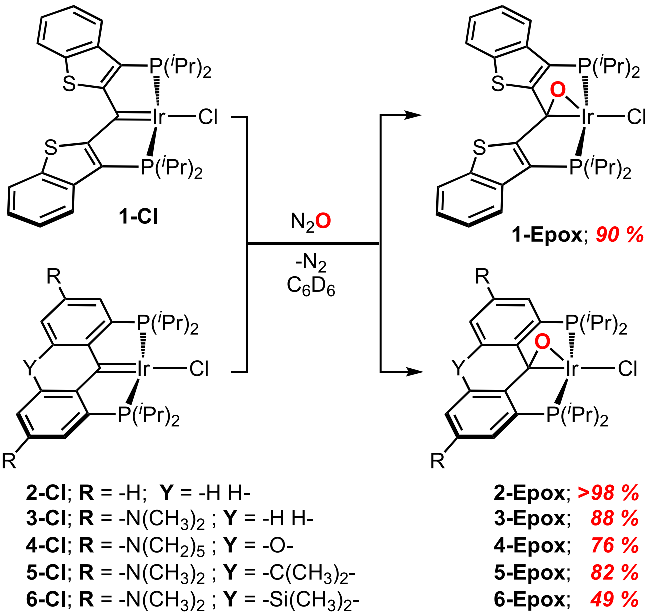

Scheme 7.

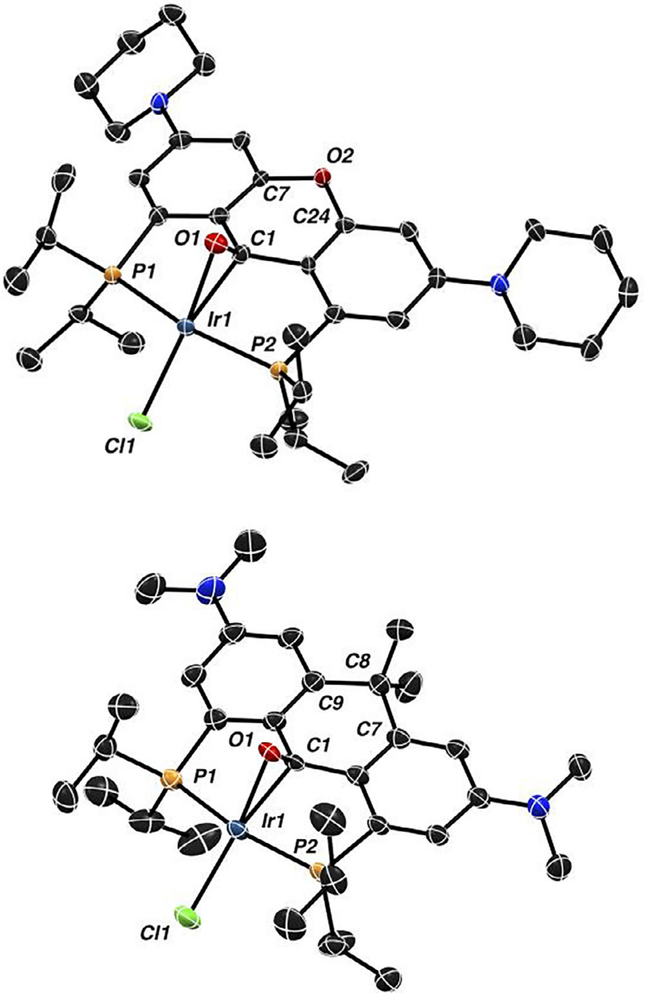

Fig. 2. Thermal ellipsoid diagrams of iridaepoxides **4-Epox** (top) and **5-Epox** (bottom) with thermal ellipsoids drawn to 50% probability. Hydrogen atoms have been omitted for clarity. Selected metrical data for **4-Epox**: Bond distances (Å): Ir1–C1, 2.069(6); Ir1–P1, 2.3317(14); Ir1–P2, 2.3267(15); Ir1–Cl1, 2.3207(14); Ir1–O1, 2.063(4); C1–O1, 1.366(7); C7–O2, 1.383(7); C24–O2, 1.379(6). Bond angles (°): P1–Ir1–P2, 160.98; C1–Ir1–Cl1, 156.46(17); Ir1–C1–O1, 70.4(3); C7–O2–C24, 117.1(4). Selected metrical data for **5-Epox**: Bond distances (Å): Ir–C1, 2.086(5); Ir1–P1, 2.2967(15); Ir1–P2, 2.3014(15); Ir1–Cl1, 2.3153(15); Ir1–O1, 2.047 (4); C1–O1, 1.352(7); C7–C8, 1.539(8); C8–C9, 1.536(9). Bond Angles (°): P1–Ir1–P2, 163.76(5); C1–Ir1–Cl, 158.68(16); Ir1–C1–O1, 69.4(3); C7–C8–C9, 112.8(5).

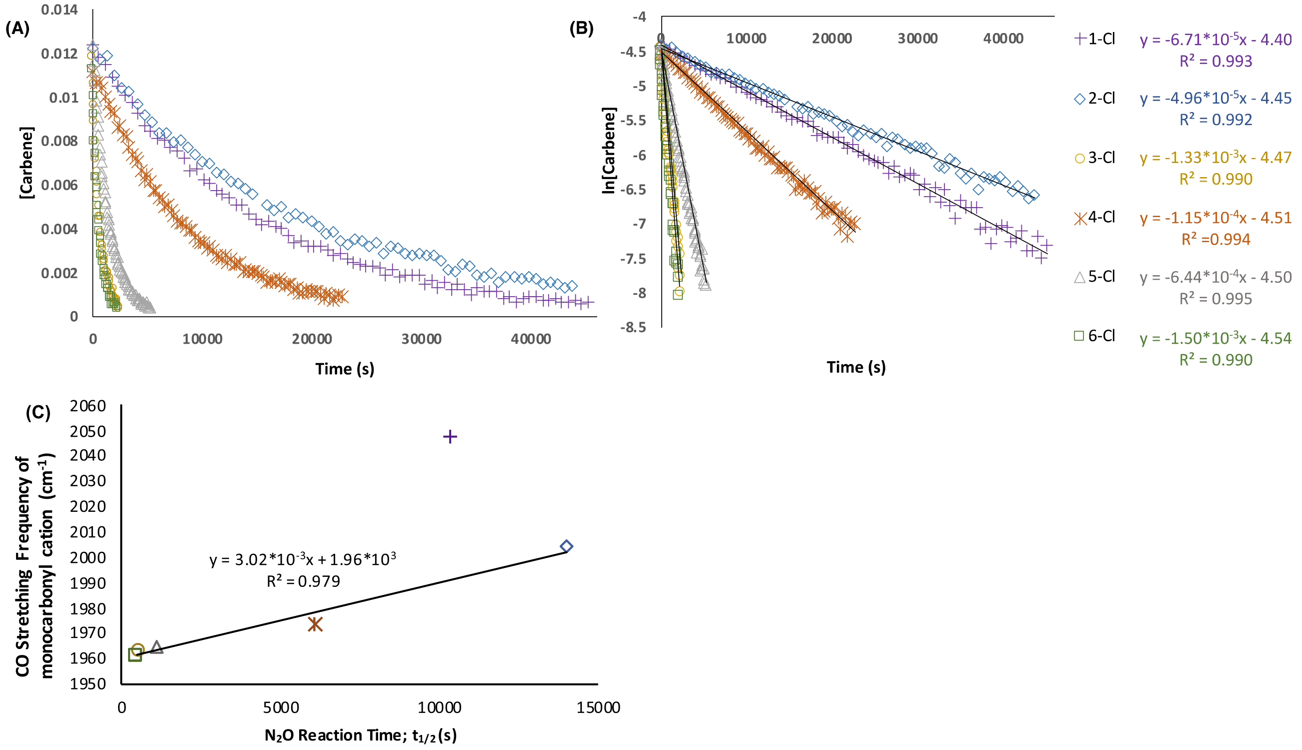

Fig. 3. (A) Decaying reaction profiles of carbene complexes **1** through **6-Cl** during reactions with N_2O at 298 K in C_6D_6. (B) Logarithmic plots of carbene concentration over time; colour coordinated pseudo-first order rate constants and R^2 values are located to the right of the legend. (C) A linear relationship between monocarbonyl ν_{CO} and half-life is depicted; outlier **1-Cl** is not included in linear regression analysis.

severely "ruffled" conformation was observed in the unlinked system **3-Epox**, which has a dihedral angle of 36.2(1)° [25].

With this library of $PC_{carbene}P$ iridium chlorides and the carbonyl stretching frequency data in hand, the relative rates of reaction with N_2O as a function of the ligand's donor properties could be assessed. Experiments were then conducted in which degassed solutions containing 0.009 mmol of a carbene complex in 0.7 mL of C_6D_6 were exposed to 1 atmosphere of N_2O at 298 K. Solubility data regarding N_2O in C_6H_6 [31] indicate that under these conditions between 0.099 mmol and 0.114 mmol of N_2O is dissolved in 0.7 mL of solution. This results in a gas to complex ratio between 11 and 13:1 which is within a *pseudo*-first order regime. Following exposure to N_2O the concentrations of starting materials and products were monitored via $^{31}P\{^1H\}$ NMR spectroscopy. Reaction profiles (Fig. 3A) show *pseudo*-first order decay at varying rates for the different carbene chloride compounds **1**-**6-Cl**. Natural logarithmic plots (Fig. 3B) confirm that this is the case with linear regression analyses providing R^2 values of >0.990. The rate of conversion to iridaepoxide products clearly increases within the series of linked compounds with strongly electron donating properties, consistent with the notion that these should more readily stabilize the formally Ir(III) iridaepoxide products. Furthermore, the rigidity of these ligand systems improves their stability towards undesired side reactions. The correlation between the rate of conversion and the donicity of the ligands is further illustrated by a plot of monocarbonyl CO stretching frequency versus half-life ($t_{1/2}$), obtained from the *pseudo* first order rate constants (Fig. 3**C**). This reveals a direct positive correlation for all complexes containing ortho-phenylene linked $PC_{carbene}P$ pincers. Quite strikingly, the outlier in these tests is the 2,3-benzo[*b*]thiophene based framework **1-Cl**. Despite the largest $\nu_{CO,}$ indicating it is the poorest overall donor, it reacted comparably to the non-functionalized parent system **2-Cl**. While the exact reasoning for this remains unknown, we speculate that the lack of steric interactions between the sulfur atoms in **1-Cl** allows the ligand to assume a more planar geometry that mimics what is seen in the rigidified systems. This feature may enhance the reaction with N_2O by making the oxygen atom transfer reaction more sterically easy than in the more flexible unlinked system **2-Cl**.

3. Conclusions

In summary, two complexes, **5-Cl** and **6-Cl**, were designed through modifications to previous ligand scaffolds to provide rigidity while maintaining a high degree of donor capability. These complexes readily reacted with N_2O to form corresponding iridaepoxides in moderate to high yields. Based on ease of synthetic accessibility, immunity to ligand decomposition and reactivity with N_2O these compounds were found to be superior to our previous systems in accepting oxygen atoms from N_2O. We are currently exploring the use of these ligands in the development of catalysts for MLC aided hydrogenation of N_2O.

4. Experimental

4.1. General Considerations.

Storage and manipulation of all compounds, unless otherwise stated, were performed under an argon atmosphere either in a VAC glove box or using a double manifold high vacuum line using standard techniques. Passage of argon through an OxisorBW scrubber (Matheson Gas Products) removed any residual oxygen and moisture. Toluene, tetrahydrofuran and hexanes were dried and purified using a Grubbs/Dow solvent purification system and stored in 500 mL thick-walled glass pressure flasks over sodium/benzophenone ketal. *n*-Pentane was purified using a M–Braun solvent purification system, dried over sodium/benzophenone ketal and stored in a 100 mL thick-walled glass pressure flask. Benzene-d_6 was dried over sodium/benzophenone ketal and stored in a 100 mL thick-walled glass pressure flask. Dichloromethane-d_2 was dried over CaH_2 and stored in a 50 mL thick-walled glass pressure flask. Acetone was dried over 3 Å molecular sieves and stored under an atmosphere of argon. All dried solvents were degassed and vacuum distilled prior to use. ^{1}H and ^{13}C NMR chemical shifts were referenced to residual solvent protons and naturally abundant ^{13}C resonances for all deuterated solvents. Chemical shift assignments are based on ^{1}H, ^{31}P{^{1}H}, ^{13}C{^{1}H}, ^{1}H–^{1}H–COSY, ^{1}H–^{13}C-HSQC, ^{1}H–^{29}SI HMBC and ^{1}H–^{13}C-HMBC NMR experiments performed on Bruker Avance III 400, Ultrashield 400, Ascend-500, or Avance-600 MHz spectrometers using TopSpin *version* 3.2 software. X-ray crystallographic analyses were performed on a Nonius system equipped with a Bruker Apex-II CCD using samples coated in Paratone 8277 oil (Exxon) and mounted on a glass fibre. Carbon monoxide gas (>99.0%) and nitrous oxide gas (99%) were purchased from Sigma-Aldrich and used without further purification. Iridium (III) chloride hydrate was purchased from Pressure Chemicals Inc. and used as received. $[Ir(COE)_2(Cl)]_2$ [32], 3,5-dibromoaniline [33] and sodium tetrakis[3,5-bis(trifluoromethyl) phenyl]borate [34] were prepared by literature methods. All other reagents were purchased from Sigma-Aldrich and used as received. Elemental and mass spectrometric analyses were performed by staff at the Instrumentation Facility in the Department of Chemistry, University of Calgary. Synthetic protocols for the synthesis of proligands **IV** and **VI** can be found in the Supplementary data.

4.2. Synthesis of **5-Cl**

To a 100 mL thick walled glass pressure vessel charged with 4,5-bis(diisopropylphosphino)-N^2,N^2,N^7,N^7,9,9-hexamethyl-9,10-dihydroanthracene-2,7-diamine (**IV**, 0.156 g, 0.296 mmol), $[Ir(COE)_2Cl]_2$ (0.132 g, 0.147 mmol) and a Teflon stirbar, toluene (10 mL) was added. The flask was sealed and the mixture was stirred at 100 °C for 15 h. The solution was cooled and filtered through a pad of celite. The filtrate was placed in a 50 mL round bottom flask and all volatiles were removed under high vacuum. The residue was sonicated in *n*–pentane (15 mL) for 20 min producing a dark powder. Using a 2 mL Büchner funnel with a fritted disc, the remaining solid was filtered off in a glovebox and washed with *n*-pentane (4 mL). A dark brownish-green solid was obtained in a 70% yield (0.156 g, 0.207 mmol). X-ray quality crystals were obtained through slow evaporation of a dilute solution of 5-Cl dissolved in benzene. ^{1}H NMR (500 MHz, C_6D_6) δ 6.70 (m, 2H, Ar**H**), 6.27 (d, $^{4}J_{HH}$ = 2.1 Hz, 2H, Ar**H**), 3.24 (m, 4H, $-PC\mathbf{H}(CH_3)_2$), 2.25 (s, 12H, $-N(C\mathbf{H}_3)_2$), 1.73 (dvt, $^{3}J_{HH}$ = 7.8 Hz, J_{HP} = 7.4 Hz, 12H, $-PCH(C\mathbf{H}_3)_2$), 1.61 (s, 6H, $-C(C\mathbf{H}_3)_2-$), 1.41 (dvt, $^{3}J_{HH}$ = 7.4 Hz, J_{HP} = 7.1 Hz, 12H, $-PCH(C\mathbf{H}_3)_2$). ^{13}C{^{1}H} NMR (126 MHz, C_6D_6) δ 194.2 (t, $^{2}J_{CP}$ = 2.9 Hz, Ir=**C**), 156.7 (vt, J_{CP} = 18.9 Hz, Ar**C**), 151.3 (vt, J_{CP} = 3.8 Hz, Ar**C**), 143.0 (vt, J_{CP} = 7.9 Hz, Ar**C**) 142.9 (vt, J_{CP} = 18.0 Hz, Ar**C**), 115.9 (s, Ar**C**H), 113.3 (s, Ar**C**H), 42.8 (s, $-\mathbf{C}(CH_3)_2-$), 40.1 (s, $-N(\mathbf{C}H_3)_2$), 28.4 (s, $-C(\mathbf{C}H_3)_2-$), 25.2 (vt, J_{CP} = 13.0 Hz, $-P\mathbf{C}H(CH_3)_2$), 20.1 (vt, J_{CP} = 2.4 Hz, $-PCH(\mathbf{C}H_3)_2$), 19.6 (s, $-PCH(\mathbf{C}H_3)_2$). ^{31}P{^{1}H} NMR (203 MHz, C_6D_6) δ 54.1 (s). Elemental *Anal.* Calc. (%) for $C_{32}H_{50}ClIrN_2P_2$: C, 51.08; H, 6.70; N, 3.72. Found: C, 51.09; H, 6.58; N, 3.62.

4.3. Synthesis of **6-Cl**

To a 100 mL thick walled glass pressure vessel charged with 1,9-bis(diisopropylphosphino)-N^3,N^3,N^7,N^7,5,5-hexamethyl-5,10-dihydrodibenzo[*b*,*e*]siline-3,7-diamine (**VI**, 0.100 g, 0.184 mmol), $[Ir(COE)_2Cl]_2$ (0.082 g, 0.092 mmol) and a Teflon stirbar, toluene (10 mL) was added. The flask was sealed and the solution was heated to 100 °C for 15 h. The solution was then heated for another 20 h under a positive flow of argon to remove any H_2 gas produced during the reaction. The solution was then filtered through a 2 mL Büchner funnel with a fritted disc. The filtrate was collected and all volatiles were removed under high vacuum. The dark residue was sonicated in *n*-pentane (5 mL) for 1 hour. The solution was filtered and a brown powder was isolated in 59% yield (0.083 g, 0.110 mmol). X-ray quality crystals were obtained by slow diffusion of *n*-pentane into a solution of 6-Cl in benzene. ^{1}H NMR (600 MHz, C_6D_6) δ 6.81 (m, 2H, Ar**H**), 6.47 (d, *J* = 2.8 Hz, 2H, Ar**H**), 3.32 (m, 4H, $-PC\mathbf{H}(CH_3)_2$), 2.19 (s, 12H, $-N(C\mathbf{H}_3)_2$), 1.73 (dvt, $^{3}J_{HH}$ = 7.9 Hz, J_{HP} = 7.5 Hz, 12H, $-PCH(C\mathbf{H}_3)_2$), 1.43 (dvt, $^{3}J_{HH}$ = 7.1 Hz, J_{HP} = 7.0 Hz, 12H, $-PCH(C\mathbf{H}_3)_2$), 0.34 (s, 6H, $-Si(C\mathbf{H}_3)_2$). ^{13}C{^{1}H} NMR (500 MHz, C_6D_6) δ 200.7 (t, J_{CP} = 2.6 Hz, Ir=**C**), 168.1 (vt, *J* = 17.0 Hz, Ar**C**), 148.9 (vt, *J* = 2.7 Hz, Ar**C**), 144.0 (vt, *J* = 16.7 Hz, Ar**C**), 134.4 (vt, *J* = 6.6 Hz, Ar**C**), 120.2 (s, Ar**C**H), 118.7 (s, Ar**C**H), 39.8 (s, $-N(\mathbf{C}H_3)_2$), 24.9 (vt, *J* = 14.0 Hz, $-P\mathbf{C}H(CH_3)_2$), 20.3 (vt, *J* = 2.2 Hz, $-PCH(\mathbf{C}H_3)_2$), 19.6 (s, $-PCH(\mathbf{C}H_3)_2$), −3.4 (s, $-Si\mathbf{C}H_3$). ^{31}P{^{1}H} NMR (203 MHz, C_6D_6) δ 47.9. ^{29}Si NMR (119 MHz, C_6D_6) δ −15.0 (determined via crosspeak in ^{1}H-^{29}Si HMBC). Elemental *Anal.* Calc. (%) for $C_{31}H_{50}ClIrN_2P_2Si$: C, 48.45; H, 6.36; N, 3.65. Found: C, 48.52; H, 6.80; N, 3.42.

4.4. Synthesis of **5-CO**

To a J-Young NMR tube charged with **5-Cl** (0.010 g, 0.013 mmol), dichloromethane (0.7 mL) was added. The vessel was sealed and the atmosphere was replaced with carbon monoxide (1 atm); the colour of the solution immediately changed from a brownish-green to dark purple. Following CO addition, the NMR tube was sealed and manually shaken for 1 s. All volatiles were removed from the J-Young NMR tube. Inside a glovebox $NaB(Ar^F)_4$ (0.014 g, 0.016 mmol) and dichloromethane (0.5 mL) were added to the purple residue. The mixture was shaken for 20 s and then filtered through glass wool into another J-Young NMR tube. All volatiles were removed *in vacuo* and the NMR tube was carefully heated with a heat gun. The residue was reconstituted with dichloromethane (1.0 mL) and the evaporation/heating process was repeated. This was performed 3 times in total, until complete conversion to the monocarbonyl cation was observed *via* ^{31}P{^{1}H} NMR. A dark purple solid was obtained with a 67% yield (0.014 g, 0.009 mmol). X-ray quality crystals were obtained by slow diffusion of *n*-pentane into a solution of **5-CO** dissolved in DCM at −20 °C. ^{1}H NMR (500 MHz, CD_2Cl_2) δ 7.72 (m, 8H, CH-*ortho*, $B(Ar^F)_4$, Ar), 7.56 (s, 4H, CH-*para*, $B(Ar^F)_4$, Ar), 6.91 (d, $^{4}J_{HH}$ = 1.9 Hz, 2H, Ar**H**), 6.88 (m, 2H, Ar**H**) 3.22 (s, 12H, $-N(C\mathbf{H}_3)_2$), 2.79 (m, 4H, $-PC\mathbf{H}(CH_3)_2$), 1.62 (s, 6H, $-C(C\mathbf{H}_3)_2-$), 1.25 (dvt, $^{3}J_{HH}$ = 9.9 Hz, J_{HP} = 7.0 Hz, 12H, $-P(CH(C\mathbf{H}_3)_2)$), 1.13 (dvt, $^{3}J_{HH}$ = 8.4 Hz, J_{HP} = 7.0 Hz, 12H, $-P(CH(C\mathbf{H}_3)_2)$). ^{13}C{^{1}H} NMR (126 MHz, CD_2Cl_2) δ 234.8 (t, $^{2}J_{CP}$ = 4.2 Hz, Ir=**C**), 195.6 (t, $^{2}J_{CP}$ = 7.3 Hz, Ir–**C**O), 162.1 (q, $^{1}J_{CB}$ = 50.0 Hz, C-B, $B(Ar^F)_4$, Ar), 155.7 (vt, J_{CP} = 4.0 Hz, Ar**C**), 152.9 (vt, J_{CP} = 18.9 Hz, Ar**C**), 152.7 (vt, J_{CP} = 6.8 Hz, Ar**C**), 144.1 (vt, J_{CP} = 17.4 Hz, Ar**C**), 135.2 (s, CH-*ortho*, $B(Ar^F)_4$, Ar), 129.2 (qq, $^{2}J_{CF}$ = 31.6 Hz, $^{4}J_{CF}$ = 3.1 Hz, $B(Ar^F)_4$, **C**-CF_3, Ar), 125.0 (q, $^{1}J_{CF}$ = 272.1 Hz, $B(Ar^F)_4$, $\mathbf{C}F_3$), 117.9 (sept, $^{3}J_{CF}$ = 4.1 Hz, CH-*para*, $B(Ar^F)_4$, Ar), 114.9 (s, Ar**C**H), 112.1 (s, Ar**C**H), 41.5 (s, $-\mathbf{C}(CH_3)_2-$), 41.1 (s, $-N(\mathbf{C}H_3)_2$), 33.6 (s, $-CH(\mathbf{C}H_3)_2-$) 27.9 (vt, J_{CP} = 14.9 Hz, $-P\mathbf{C}H(CH_3)_2$), 19.3 (vt, J_{CP} = 2.4 Hz, $-PCH(\mathbf{C}H_3)_2$), 17.7 (s, $-PCH(\mathbf{C}H_3)_2$). ^{31}P{^{1}H} NMR (203 MHz, CD_2Cl_2) δ 71.8 (s). ^{19}F{^{1}H} NMR (471 MHz, CD_2Cl_2) δ −63.85 (s). ^{11}B{^{1}H} NMR (161 MHz, CD_2Cl_2) δ −6.05 (s). IR (AgCl plates) cm^{-1}: 1965 (s). ESI-MS (M*+) for $[C_{33}H_{50}IrN_2OP_2]^+$ $[C_{32}H_{12}BF_{24}]^-$: Calcd.: 745.3022. Found: 745.3013.

4.5. Synthesis of **6-CO**

In a J-Young NMR tube **6-Cl** (0.010 g, 0.013 mmol) was dissolved in DCM (0.7 mL). The vessel was sealed and the atmosphere was replaced with carbon monoxide (1 atm); the colour of the solution immediately changed from a brownish-green to dark purple. Following CO addition, the NMR tube was sealed and manually shaken for 1 s. All volatiles were removed from the J-Young NMR tube. Inside a glovebox NaB(Ar^F)$_4$ (0.020 g, 0.023 mmol) and dichloromethane (0.5 mL) were added to the purple residue. The solution was mixed for 20 s and then filtered through glass wool into another J-Young NMR tube. All volatiles were removed *in vacuo* and the NMR tube was carefully heated with a heat gun. The residue was reconstituted with dichloromethane (1.0 mL) and the evaporation/heating process was repeated. This was performed 4 times in total, until complete conversion to the monocarbonyl cation was observed *via* ^{31}P{^{1}H} NMR. A blue solid was isolated in 90% yield (0.019 g, 0.012 mmol). ^{1}H NMR (400 MHz, CD$_2$Cl$_2$) δ 7.72 (m, 8H, CH-*ortho*, B(Ar^F)$_4$, Ar), 7.56 (s, 4H, CH-*para*, B(Ar^F)$_4$, Ar), 7.03 (d, $^4J_{HH}$ = 2.8 Hz, 2H, ArC**H**), 6.88 (m, 2H, ArC**H**), 3.21 (s, 12H, –N(C**H**$_3$)$_2$), 2.78 (m, 4H, –PC**H**(CH$_3$)$_2$), 1.25 (dvt, $^3J_{HH}$ = 7.1 Hz, J_{HP} = 9.9 Hz, 12H, –PCH(C**H**$_3$)$_2$), 1.13 (dvt, $^3J_{HH}$ = 7.1 Hz, J_{HP} = 8.5 Hz 12H, –PCH(C**H**$_3$)$_2$), 0.43 (s, 6H, –Si(C**H**$_3$)$_2$). ^{13}C{^{1}H} NMR (101 MHz, CD$_2$Cl$_2$) δ 250.5 (t, $^2J_{CP}$ = 4.0 Hz, Ir═**C**), 193.7 (t, J_{CP} = 8.1 Hz, Ir–**C**O), 162.1 (q, $^1J_{CB}$ = 50.0 Hz, C-B, B(Ar^F)$_4$, ArC), 156.2 (vt, J_{CP} = 17.1 Hz, Ar**C**), 152.6 (vt, J_{CP} = 3.8 Hz, Ar**C**), 152.2 (vt, J_{CP} = 15.3 Hz, Ar**C**), 145.0 (vt, J_{CP} = 5.5 Hz, Ar**C**), 135.2 (s, CH-*ortho*, B(Ar^F)$_4$, Ar**C**), 129.3 (qq, $^2J_{CF}$ = 31.5 Hz, $^4J_{CF}$ = 2.7 Hz, **C**-CF$_3$, B(Ar^F)$_4$), 125.0 (q, $^1J_{CF}$ = 272.4 Hz, **C**F$_3$, B(Ar^F)$_4$), 120.9 (s, Ar**C**H), 117.9 (sept, $^3J_{CF}$ = 4.0 Hz, CH-*para*, B(Ar^F)$_4$, Ar), 116.5 (s, Ar**C**H), 40.9 (s, –N(**C**H$_3$)$_2$), 27.2 (vt, J_{CP} = 15.1 Hz, –P**C**H(CH$_3$)$_2$), 19.7 (s –PCH(**C**H$_3$)$_2$), 19.3 (s, –PCH(**C**H$_3$)$_2$), −1.3 (s, –Si(**C**H$_3$)$_2$). ^{31}P{^{1}H} NMR (162 MHz, CD$_2$Cl$_2$) δ 68.4. ^{19}F{^{1}H} NMR (376 MHz, CD$_2$Cl$_2$) δ −59.3. ^{11}B{^{1}H} NMR (128 MHz, CD$_2$Cl$_2$) δ −7.0. ^{29}Si NMR (119 MHz, CD$_2$Cl$_2$) δ −19.5 (determined via crosspeak in ^{1}H-^{29}Si HMBC). IR (AgCl plates) cm^{-1}: 1961(s). ESI-MS (M*+) for [C$_{32}$H$_{50}$IrN$_2$OP$_2$Si]$^+$ [C$_{32}$H$_{12}$BF$_{24}$]$^-$: Calcd.:761.2791; Found: 761.2790.

4.6. Synthesis of 5-(CO)$_2$

To a J-Young NMR tube charged with **5-Cl** (0.010 g, 0.013 mmol), dichloromethane (0.7 mL) was added. The vessel was sealed and the atmosphere was replaced with carbon monoxide (1 atm); the colour of the solution immediately changed from a brownish-green to dark purple. Following CO addition the NMR tube was sealed and manually shaken for 3 s. All volatiles were removed from the J-Young NMR tube immediately. Inside a glovebox NaB(Ar^F)$_4$ (0.014 g, 0.016 mmol) and dichloromethane (0.5 mL) were added to the purple residue. The mixture was shaken for ~10 s and then filtered through glass wool into another J-Young NMR tube. The atmosphere of the NMR tube was replaced with CO (1 atm) and shaken for 10 s. All volatiles were removed *in vacuo* and a dark purple solid was obtained with a 75% yield (0.016 g, 0.010 mmol). ^{1}H NMR (500 MHz, CD$_2$Cl$_2$) δ 7.72 (m, 8H, CH-*ortho*, B(Ar^F)$_4$, Ar), 7.56 (s, 4H, CH-*para*, B(Ar^F)$_4$, Ar), 6.81 (d, $^4J_{HH}$ = 1.9 Hz, 2H, Ar**H**), 6.77 (m, 2H, Ar**H**) 3.12 (s, 12H, –N(C**H**$_3$)$_2$), 2.76 (m, 4H, –PC**H**(CH$_3$)$_2$), 1.64 (s, 6H, –C(C**H**$_3$)$_2$–), 1.20 (dvt, $^3J_{HH}$ = 10.5 Hz, J_{HP} = 7.1 Hz, 12H, –PCH(C**H**$_3$)$_2$), 1.13 (dvt, $^3J_{HH}$ = 9.1 Hz, J_{HP} = 7.1 Hz, 12H, –PCH(C**H**$_3$)$_2$). ^{13}C{^{1}H} NMR (151 MHz, CD$_2$Cl$_2$) δ 226.1 (t, $^2J_{CP}$ = 4.8 Hz, Ir═**C**), 179.1 (t, $^2J_{CP}$ = 5.2 Hz, Ir–**C**O), 162.2 (q, ^{1}J$_{CB}$ = 49.9 Hz, C-B, B(Ar^F)$_4$, Ar), 153.3 (vt, J_{CP} = 4.2 Hz, Ar**C**), 147.5 (vt, J_{CP} = 7.9 Hz, Ar**C**), 145.4 (vt, J_{CP} = 22.4 Hz, Ar**C**), 144.5 (vt, J_{CP} = 16.7 Hz, Ar**C**), 135.3 (s, CH-*ortho*, B(Ar^F)$_4$, Ar), 129.4 (qq, $^2J_{CF}$ = 31.3 Hz, $^4J_{CF}$ = 2.7 Hz, B(Ar^F)$_4$, **C**-CF$_3$, Ar), 125.1 (q, $^1J_{CF}$ = 271.8 Hz, B(Ar^F)$_4$, **C**F$_3$), 117.9 (sept, $^3J_{CF}$ = 3.9 Hz, CH-*para*, B(Ar^F)$_4$, Ar), 115.0 (s, Ar**C**H), 112.3 (s, Ar**C**H), 41.1 (s, –**C**(CH$_3$)$_2$–), 40.8 (s, –N(**C**H$_3$)$_2$), 32.9 (s, –CH(**C**H$_3$)$_2$–) 27.9 (vt, J_{CP} = 15.8 Hz, –PCH(**C**H$_3$)$_2$), 19.3 (s, –PCH(**C**H$_3$)$_2$), 17.7 (s, –PCH(**C**H$_3$)$_2$).^{31}P{^{1}H} NMR (203 MHz, CD$_2$Cl$_2$) δ 58.8 (s). ^{19}F{^{1}H} NMR (471 MHz, CD$_2$Cl$_2$) δ −63.84 (s). ^{11}B{^{1}H} NMR (161 MHz, CD$_2$Cl$_2$) δ −6.05 (s). IR (AgCl plates) cm^{-1}: 2014 (s), 1974 (s). Elemental *Anal.* Calc. (%) for C$_{66}$H$_{62}$BF$_{24}$IrN$_2$O$_2$P$_2$: C, 48.45; H, 3.82; N, 1.71. Found: C, 48.26; H, 3.86; N, 1.67.

4.7. Synthesis of 6-(CO)$_2$

To a thick-walled glass pressure vessel (25 mL) charged with a Teflon stirbar, **6-Cl** (0.020 g, 0.026 mmol) was dissolved in dichloromethane (3 mL). The solution was degassed at room temperature and placed under 1 atm. of carbon monoxide, immediately turning purple. The mixture was stirred for 5 s and then all volatiles were removed. NaB(Ar^F)$_4$ (0.050 g, 0.056 mmol) was added to the flask along with DCM (3 mL). This mixture was stirred for 30 s at room temperature and then filtered through celite into another flask (25 mL). The solution was again placed under 1 atm of CO and stirred for 5 s. All volatiles were removed and a dark purple solid was isolated in 83% yield (0.035 g, 0.021 mmol).^{1}H NMR (500 MHz, CD$_2$Cl$_2$) δ 7.73 (m, 8H, CH-*ortho*, B(Ar^F)$_4$, Ar), 7.57 (s, 4H, CH-*para*, B(Ar^F)$_4$, Ar), 6.91 (d, $^4J_{HH}$ = 2.9 Hz, 2H, ArC**H**), 6.80 (m, 2H, ArC**H**), 3.09 (s, 12H, –N(C**H**$_3$)$_2$), 2.76 (m, 4H, –PC**H**(CH$_3$)$_2$), 1.23 (dvt, $^3J_{HH}$ = 7.2 Hz, J_{HP} = 10.7 Hz, 12H, –PCH(C**H**$_3$)$_2$), 1.10 (dvt, $^3J_{HH}$ = 6.9 Hz, J_{HP} = 9.4 Hz, 12H, –PCH(C**H**$_3$)$_2$), 0.42 (s, 6H, –Si(C**H**$_3$)$_2$). ^{13}C{^{1}H} NMR (500 MHz, CD$_2$Cl$_2$) δ 240.6 (t, $^2J_{CP}$ = 4.4 Hz, Ir═**C**), 180.4 (t, $^2J_{CP}$ = 4.9 Hz, Ir–**C**O), 162.2 (q, $^1J_{CB}$ = 50.1 Hz, C-B, B(Ar^F)$_4$, Ar), 153.5 (vt, J_{CP} = 13.4 Hz, Ar**C**), 150.3 (vt, J_{CP} = 3.9 Hz, Ar**C**), 147.9 (vt, J_{CP} = 21.5 Hz, Ar**C**), 139.5 (vt, J_{CP} = 6.3 Hz, Ar**C**), 135.2 (s, CH-*ortho*, B(Ar^F)$_4$, Ar), 129.3 (qq, $^2J_{CF}$ = 31.5 Hz, $^4J_{CF}$ = 2.7 Hz, **C**-CF$_3$, B(Ar^F)$_4$, Ar), 125.0 (q, $^1J_{CF}$ = 272.2 Hz, **C**F$_3$, B(Ar^F)$_4$), 119.7 (s, Ar**C**H), 117.9 (sept, $^3J_{CF}$ = 4.0 Hz, CH-*para*, B(Ar^F)$_4$, Ar), 116.7 (s, Ar**C**H), 40.6 (s, –N(**C**H$_3$)$_2$), 28.5 (vt, J_{CP} = 15.7 Hz, –P**C**H(CH$_3$)$_2$), 19.4 (s –PCH(**C**H$_3$)$_2$), 17.9 (s, –PCH(**C**H$_3$)$_2$), −1.5 (s, –Si(**C**H$_3$)$_2$). ^{31}P{1H} NMR (162 MHz, CD$_2$Cl$_2$) δ 55.0. ^{19}F{^{1}H} NMR (376 MHz, CD$_2$Cl$_2$) δ −63.9. ^{11}B{^{1}H} NMR (128 MHz, CD$_2$Cl$_2$) δ −6.1. ^{29}Si{^{1}H} NMR (119 MHz, CD$_2$Cl$_2$) δ −20.3 (determined via crosspeak in ^{1}H-^{29}Si HMBC). IR (AgCl plates) cm^{-1}: 2018 (s) and 1971 (s). Elemental *Anal.* Calc. (%) for C$_{65}$H$_{62}$BF$_{24}$IrN$_2$O$_2$P$_2$Si: C, 47.25; H, 3.78; N, 1.70. Found: C, 47.14; H, 3.46; N, 1.57.

4.8. Synthesis of 2-Epox

To a J-Young NMR tube charged with **2-Cl** (0.007 g, 0.011 mmol), C$_6$D$_6$ was added. The solution was degassed, placed under 1 atm. of N$_2$O and mixed at room temperature for 24 h. All volatiles were removed *in vacuo* and the remaining residue was sonicated in *n*-pentane (1 mL) until a powder formed. The *n*-pentane was removed under high vacuum and dried for 10 min. A red–orange solid was isolated with >98% yield (0.007 g, 0.011 mmol).^{1}H NMR (400 MHz, C$_6$D$_6$) δ 7.85 (d, J_{HH} = 7.3 Hz, 2H, Ar**H**), 7.09 (m, 2H, Ar**H**), 7.04 (m, 2H, Ar**H**), 6.88 (t, J_{HH} = 7.6 Hz 2H, Ar**H**), 2.94 (m, 2H, –PC**H**(CH$_3$)$_2$), 2.48 (s, 2H, –PC**H**(CH$_3$)$_2$), 1.46 (dvt, $^3J_{HH}$ = 7.6 Hz, J_{HP} = 7.6 Hz, 6H, –PCH(C**H**$_3$)$_2$), 1.37 (dvt, $^3J_{HH}$ = 7.9 Hz, J_{HP} = 8.0 Hz, 6H, –PCH(C**H**$_3$)$_2$), 1.26 (dvt, $^3J_{HH}$ = 7.9 Hz, J_{HP} = 7.7 Hz, 6H, –PCH(C**H**$_3$)$_2$), 1.11 (dvt, $^3J_{HH}$ = 6.8 Hz, J_{HP} = 7.1 Hz, 6H, –PCH(C**H**$_3$)$_2$),. ^{13}C{^{1}H} NMR (101 MHz, C$_6$D$_6$) δ 152.0 (s, Ar**C**), 132.9 (s, Ar**C**H), 132.4 (vt, J_{CP} = 19.2 Hz, Ar**C**), 128.8 (s, Ar**C**H), 126.7 (vt, J_{CP} = 3.1 Hz, Ar**C**H), 126.4 (vt, J_{CP} = 5.4 Hz, Ar**C**H) 81.7 (t, J_{CP} = 2.5 Hz, Ir(O)**C**), 24.3 (vt, J_{CP} = 13.9 Hz, –P**C**H(CH$_3$)$_2$), 23.5 (vt, J_{CP} = 14.1 Hz, –P**C**H(CH$_3$)$_2$), 20.4 (vt, J_{CP} = 2.6 Hz, –PCH(**C**H$_3$)$_2$), 19.1 (vt, J_{CP} = 1.7 Hz, –PCH(**C**H$_3$)$_2$), 18.4 (vt, J_{CP} = 2.3 Hz, –PCH(**C**H$_3$)$_2$), 17.2 (s, –PCH(**C**H$_3$)$_2$).^{31}P{^{1}H} NMR (162 MHz, C$_6$D$_6$) δ 28.5. ESI-MS (M + H) for C$_{25}$H$_{36}$IrOP$_2$: Calcd: 643.1632. Found: 643.1621.

4.9. Synthesis of 4-Epox

To a 25 mL thick walled glass pressure vessel charged with **4-Cl** (0.128 g, 0.159 mmol) and a teflon stirbar, toluene (5 mL) was added. The flask was degassed, placed under 1 atm. of N$_2$O and stirred at 80 °C for 1 hour. Toluene was removed *in vacuo* and the remaining residue was sonicated in *n*-pentane (10 mL). The resultant red powder was filtered and washed with *n*-pentane (3 x 2 mL). The red–orange solid was dried under high vacuum at room temperature for 2 h and isolated with an 88% yield (0.115 g, 0.140 mmol). X-ray quality crystals were obtained by slow diffusion of *n*-pentane into a solution of **4-Epox** dissolved in benzene.^{1}H NMR (500 MHz, C$_6$D$_6$) δ 6.81 (m, 2H, Ar**H**), 6.60 (d, J = 1.9 Hz, 2H, Ar**H**), 3.11 (m, 2H, –PC**H**(CH$_3$)$_2$), 2.93–2.85 (m, 8H, N(C**H**$_2$)$_5$), 2.43 (m, 2H, –PC**H**(CH$_3$)$_2$), 1.45 (dvt, J_{HP} = 7.6 Hz, J_{HH} = 8.29 Hz 6H, –PCH(C**H**$_3$)$_2$), 1.43 – 1.35 (m, –PCH(C**H**$_3$)$_2$, N(C**H**$_2$)$_5$), 1.29 – 1.24 (m, N(C**H**$_2$)$_5$), 1.22 (dvt, J_{HP} = 6.8 Hz, J_{HH} = 6.7 Hz, –PCH(C**H**$_3$)$_2$) (region between 1.48 and 1.16 integrates to 36H). ^{13}C{^{1}H } NMR (126 MHz, C$_6$D$_6$) δ 153.6 (vt, J_{CP} = 4.5 Hz, Ar**C**), 152.5 (vt, J_{CP} = 8.0 Hz, Ar**C**), 132.0 (vt, J_{CP} = 18.6 Hz, Ar**C**), 128.3 (Ar**C**, seen using ^{1}H–^{13}C HMBC), 114.9 (s, Ar**C**H), 104.6 (s, Ar**C**H), 72.3 (t, J_{CP} = 3.2 Hz, Ir(O)**C**), 50.8 (s, N(**C**H$_2$)$_5$), 25.9 (s, N(**C**H$_2$)$_5$), 25.0 (vt, J_{CP} = 12.4 Hz, –P**C**H(CH$_3$)$_2$), 24.5 (s, N(**C**H$_2$)$_5$), 23.0 (vt, J_{CP} = 14.3 Hz, –P**C**H(CH$_3$)$_2$), 19.9 (vt, J_{CP} = 1.8 Hz, –PCH(**C**H$_3$)$_2$), 19.1 (s, –PCH(**C**H$_3$)$_2$), 18.8 (vt, J_{CP} = 3.2 Hz, –PCH(**C**H$_3$)$_2$), 17.6 (s, –PCH(**C**H$_3$)$_2$). ^{31}P{^{1}H} NMR (203 MHz, C$_6$D$_6$) δ 30.0 (s). Elemental *Anal.* Calc. (%) for C$_{35}$H$_{52}$ClIrN$_2$O$_2$P$_2$: C, 51.12; H, 6.37; N, 3.41 Found: C, 50.91; H, 6.53; N, 3.38.

4.10. Synthesis of 5-Epox

To a 50 mL thick walled glass pressure vessel charged with **5-Cl** (0.098 g, 0.130 mmol) and a Teflon stirbar, benzene (10 mL) was added. The flask was degassed, placed under 1 atm. of N$_2$O, sealed and stirred at 80 °C for 1 hour. All volatiles were removed under high vacuum. The red residue was sonicated in *n*-pentane (10 mL). The resultant red powder was filtered and washed with *n*-pentane (3 x 2 mL). The solid was dried under high vacuum for 2 h at 80 °C to give a pale red powder in 76% yield (0.076 g, 0.099 mmol). X-ray quality crystals were obtained through slow evaporation of a dilute solution of **5-Epox** dissolved in benzene.^{1}H NMR (500 MHz, C$_6$D$_6$) δ 6.72 (m, 4H, Ar**H**), 3.25 (m, 2H, –PC**H**(CH$_3$)$_2$), 2.58 (s, 12H, –N(C**H**$_3$)$_2$), 2.52 (m, 2H, –PC**H**(CH$_3$)$_2$), 1.77 (s, 3H, –C(C**H**$_3$)$_2$–), 1.56 (s, 3H, –C(C**H**$_3$)$_2$–), 1.51 (dvt, $^{3}J_{HH}$ = 7.7 Hz, J_{HP} = 7.6 Hz, 6H, –PCH(C**H**$_3$)$_2$), 1.43 (m, 12H, –PCH(C**H**$_3$)$_2$), 1.30 (dvt, $^{3}J_{HH}$ = 6.7 Hz, J_{HP} = 6.7 Hz, 6H, –PCH(C**H**$_3$)$_2$).^{13}C{^{1}H } NMR (126 MHz, C$_6$D$_6$) δ 150.1 (vt, J_{CP} = 4.0 Hz, Ar**C**), 145.1 (vt, J_{CP} = 6.1 Hz, Ar**C**), 137.4 (vt, J_{CP} = 9.1 Hz, Ar**C**) 131.1 (vt, J_{CP} = 19.2 Hz, Ar**C**), 114.19 (s, Ar**C**H), 111.0 (s, Ar**C**H), 79.5 (t, $^{2}J_{CP}$ = 3.3 Hz, Ir(O)**C**), 40.4 (s, –N(**C**H$_3$)$_2$), 39.3 (s, –**C**(CH$_3$)$_2$–), 36.8 (s, –C(**C**H$_3$)$_2$), 29.70 (s, –C(**C**H$_3$)$_2$), 25.0 (vt, J_{CP} = 12.7 Hz, –P**C**H(CH$_3$)$_2$), 22.5 (vt, J_{CP} = 14.9 Hz, –P**C**H(CH$_3$)$_2$), 20.0 (vt, J_{CP} = 2.0 Hz, –PCH(**C**H$_3$)$_2$), 19.36 (s, –PCH(**C**H$_3$)$_2$), 18.6 (vt, J_{CP} = 3.0 Hz, –PCH(**C**H$_3$)$_2$), 17.4 (s, –PCH(**C**H$_3$)$_2$).^{31}P{^{1}H} NMR (203 MHz, C$_6$D$_6$) δ 28.5 (s). Elemental *Anal.* Calc. (%) for C$_{32}$H$_{50}$ClIrN$_2$OP$_2$: C, 50.02; H, 6.56; N, 3.65. Found: C, 50.45; H, 6.58; N, 3.44.

4.11. Synthesis of 6-Epox

To a J-Young NMR tube charged with **6-Cl** (0.020 g, 0.026 mmol, toluene (5 mL) was added. The tube was degassed, placed under 1 atm. of N$_2$O and mixed at room temperature for 3 h. All volatiles were removed *in vacuo* and the remaining residue was sonicated in *n*-pentane (1.5 mL). The resultant red powder was filtered, dried under high vacuum at room temperature for 20 min and isolated with a 49% yield (0.010 g, 0.013 mmol). ^{1}H NMR (400 MHz, C$_6$D$_6$) δ 6.82 (m, 2H, Ar**H**), 6.79 (d, $^{4}J_{HH}$ = 2.47 Hz, 2H, Ar**H**), 3.31 (m, 2H, –PC**H**(CH$_3$)$_2$), 2.56 (s, 12H (14H with δ 2.54), –N(C**H**$_3$)$_2$), 2.54 (m, 2H (14H with δ 2.56), –PC**H**(CH$_3$)$_2$), 1.73 (dvt, $^{3}J_{HH}$ = 7.9 Hz, J_{HP} = 7.4 Hz, 6H, –PCH(C**H**$_3$)$_2$), 1.43 (m, 12H –PCH(C**H**$_3$)$_2$), 1.29 (dvt, $^{3}J_{HH}$ = 6.5 Hz, J_{HP} = 6.6 Hz, 6H, –PCH(C**H**$_3$)$_2$), 0.48 (s, 3H, –Si(C**H**$_3$)$_2$), 0.32 (s, 3H, –Si(C**H**$_3$)$_2$). ^{13}C{^{1}H} NMR (101 MHz, C$_6$D$_6$) δ 148.2 (vt, J_{CP} = 3.4 Hz, Ar**C**), 147.2 (vt, J_{CP} = 7.8 Hz, Hz, Ar**C**), 134.0 (vt, J_{CP} = 4.9 Hz, Ar**C**), 131.7 (vt, J_{CP} = 17.5 Hz, Ar**C**), 117.6 (s, Ar**C**H), 117.5 (s, Ar**C**H), 83.6 (t, $^{2}J_{CP}$ = 2.7 Hz, Ir(O)**C**), 40.0 (s, –N(**C**H$_3$)$_2$), 25.0 (vt, J = 12.9 Hz, –P**C**H(CH$_3$)$_2$), 22.0 (vt, J_{CP} = 14.4 Hz, –P**C**H(CH$_3$)$_2$), 20.0 (vt, J_{CP} = 1.8 Hz, –PCH(**C**H$_3$)$_2$), 19.6 (s, –PCH(**C**H$_3$)$_2$), 18.6 (vt, J_{CP} = 3.0 Hz –PCH(**C**H$_3$)$_2$), 17.3 (s, –PCH(**C**H$_3$)$_2$), −0.7 (s, –Si**C**H$_3$), −1.7 (s, –Si**C**H$_3$). ^{31}P{^{1}H} NMR (162 MHz, C$_6$D$_6$) δ 27.6. ^{29}Si NMR (80 MHz, C$_6$D$_6$) δ −21.5 (determined via crosspeak in ^{1}H-^{29}Si HMBC). Elemental *Anal.* Calc. (%) for C$_{31}$H$_{50}$ClIrN$_2$OP$_2$Si: C, 47.47; H, 6.42; N, 3.57. Found: C, 47.47; H, 6.34; N, 6.43.

Acknowledgement

Funding for this work was provided by NSERC of Canada in the form of a Discovery Grant to W.E.P. W.E.P also thanks the Canada Research Chair secretariat for a Tier **I** CRC (2013-2020). J.D.S. thanks NSERC for a PGSD scholarship.

Appendix A. Supplementary data

CCDC 1852330-34 contains the supplementary crystallographic data for **4-Epox**, **5-Cl**, **5-CO**, **5-Epox** and **6-C**. These data can be obtained free of charge via http://www.ccdc.cam.ac.uk/conts/retrieving.html, or from the Cambridge Crystallographic Data Centre, 12 Union Road, Cambridge CB2 1EZ, UK; fax: (+44) 1223-336-033; or e-mail: deposit@ccdc.cam.ac.uk.

Supplementary data associated with this article can be found, in the online version, at https://doi.org/10.1016/j.poly.2018.08.054.

References

[1] C.J. Moulton, B.L. Shaw, Transition metal-carbon bonds. Part XLII. Complexes of nickel, palladium, platinum, rhodium and iridium with the tridentate ligand 2,6-bis[(di-t-butylphosphino)methyl]phenyl, J. Chem. Soc., Dalton Trans. (1976) 1020.

[2] G. van Koten, D. Milstein, Organometallic Pincer, Chemistry, Springer, Berlin; New York, 2013.

[3] J. Choi, A.H.R. MacArthur, M. Brookhart, A.S. Goldman, Dehydrogenation and related reactions catalyzed by iridium pincer complexes, Chem. Rev. 111 (2011) 1761.

[4] N.A. Eberhardt, H. Guan, Chapter 4 – reduction of CO2 mediated or catalyzed by pincer complexes, in: D. Morales-Morales (Ed.), Pincer Compounds, Elsevier, 2018, pp. 67–99.

[5] E. Peris, R.H. Crabtree, Key factors in pincer ligand design, Chem. Soc. Rev. 47 (2018) 1959.

[6] G.V. Koten, Pure Appl. Chem. 61 (1989) 1681.

[7] D. Hermann, M. Gandelman, H. Rozenberg, L.J.W. Shimon, D. Milstein, Synthesis, structure, and reactivity of new rhodium and iridium complexes, bearing a highly electron-donating PNP system. Iridium-mediated vinylic C-H bond activation, Organometallics 21 (2002) 812.

[8] J.R. Khusnutdinova, D. Milstein, Metal-Ligand Cooperation, Angew. Chem.-Int. Ed. 54 (2015) 12236.

[9] C. Gunanathan, D. Milstein, Metal-ligand cooperation by aromatization-dearomatization: a new paradigm in bond activation and "green" catalysis, Acc. Chem. Res. 44 (2011) 588.

[10] M. Feller, U. Gellrich, A. Anaby, Y. Diskin-Posner, D. Milstein, Reductive cleavage of CO2 by metal–ligand-cooperation mediated by an iridium pincer complex, J. Am. Chem. Soc. 138 (2016) 6445.

[11] D.V. Gutsulyak, W.E. Piers, J. Borau-Garcia, M. Parvez, Activation of water, ammonia, and other small molecules by PC carbeneP nickel pincer complexes, J. Am. Chem. Soc. 135 (2013) 11776.

[12] W.B. Tolman, Binding and activation of N2O at transition-metal centers: Recent mechanistic insights, Angew. Chem.-Int. Ed. 49 (2010) 1018.

[13] A.R. Ravishankara, J.S. Daniel, R.W. Portmann, Nitrous oxide (N2O): The dominant ozone-depleting substance emitted in the 21st century, Science 326 (2009) 123.

[14] J.H. Lee, M. Pink, J. Tomaszewski, H. Fan, K.G. Caulton, Facile hydrogenation of N2O by an operationally unsaturated osmium polyhydride, J. Am. Chem. Soc. 129 (2007) 8706.

[15] A.W. Kaplan, R.G. Bergman, Nitrous oxide mediated synthesis of monomeric hydroxoruthenium complexes. Reactivity of (DMPE)2Ru(H)(OH) and the synthesis of a silica-bound ruthenium complex, Organometallics 17 (1998) 5072.

[16] A.W. Kaplan, R.G. Bergman, Nitrous oxide mediated oxygen atom insertion into a ruthenium–hydride bond. Synthesis and reactivity of the monomeric hydroxoruthenium complex (DMPE)2Ru(H)(OH), Organometallics 16 (1997) 1106.

[17] T.L. Gianetti, S.P. Annen, G. Santiso-Quinones, M. Reiher, M. Driess, H. Grützmacher, Nitrous oxide as a hydrogen acceptor for the dehydrogenative coupling of alcohols, Angew. Chem.-Int. Ed. 55 (2016) 1854.

[18] T.L. Gianetti, R.E. Rodríguez-Lugo, J.R. Harmer, M. Trincado, M. Vogt, G. Santiso-Quinones, H. Grützmacher, Zero-valent amino-olefin cobalt complexes as catalysts for oxygen atom transfer reactions from nitrous oxide, Angew. Chem.-Int. Ed. 55 (2016) 15323.

[19] R. Zeng, M. Feller, Y. Ben-David, D. Milstein, Hydrogenation and hydrosilylation of nitrous oxide homogeneously catalyzed by a metal complex, J. Am. Chem. Soc. 139 (2017) 5720.

[20] J. Arras, H. Speth, H.A. Mayer, L. Wesemann, Different Coordination Modes of the $Ph_2PC_{sp3}PPh_2$ pincer ligand in rhodium complexes as a consequence of C_{sp3}-H metal interaction, Organometallics 34 (2015) 3629.

[21] J.R. Logan, W.E. Piers, J. Borau-Garcia, D.M. Spasyuk, Ligand attachment chemistry in the preparation of PCsp 3P and PCsp 2P complexes of rhodium, Organometallics 35 (2016) 1279.

[22] R.J. Burford, W.E. Piers, M. Parvez, β-Elimination-immune PC carbeneP iridium complexes via double C-H activation: ligand-metal cooperation in hydrogen activation, Organometallics 31 (2012) 2949.

[23] L.E. Doyle, W.E. Piers, J. Borau-Garcia, Ligand cooperation in the formal hydrogenation of N2O using a PC(sp2)P iridium pincer complex, J. Am. Chem. Soc. 137 (2015) 2187.

[24] L.E. Doyle, W.E. Piers, J. Borau-Garcia, M.J. Sgro, D.M. Spasyuk, Mechanistic studies on the addition of hydrogen to iridaepoxide complexes with subsequent elimination of water, Chem. Sci. 7 (2016) 921.

[25] J.D. Smith, J. Borau-Garcia, W.E. Piers, D. Spasyuk, Systematic dismantling of a carefully designed PCcarbeneP pincer ligand via C-C bond activations at an iridium centre, Can. J. Chem. 94 (2016) 293.

[26] J.D. Smith, J.R. Logan, L.E. Doyle, R.J. Burford, S. Sugawara, C. Ohnita, Y. Yamamoto, W.E. Piers, D.M. Spasyuk, J. Borau-Garcia, Cationic mono and dicarbonyl pincer complexes of rhodium and iridium to assess the donor properties of PCcarbeneP ligands, Dalton Trans. 45 (2016) 12669.

[27] T. Pastierik, P. Sebej, J. Medalova, P. Stacko, P. Klan, Near-infrared fluorescent 9-phenylethynylpyronin analogues for bioimaging, J. Org. Chem. 79 (2014) 3374.

[28] G. Lukinavičius, K. Umezawa, N. Olivier, A. Honigmann, G. Yang, T. Plass, V. Mueller, L. Reymond, I.R. Corrêa Jr, Z.G. Luo, C. Schultz, E.A. Lemke, P. Heppenstall, C. Eggeling, S. Manley, K. Johnsson, A near-infrared fluorophore for live-cell super-resolution microscopy of cellular proteins, Nat. Chem. 5 (2013) 132.

[29] L.J. Gu, B.Q. Yang, F.L. Liu, Y.J. Bai, Efficient synthetic route to carbopyronine fluorenscent dye intermediate, Chin. J. Chem . 27 (2009) 1199.

[30] H. Werner, Carbene-Transition metal complexes formed by double C-H bond activation, Angew. Chem.-Int. Ed. 49 (2010) 4714.

[31] L.C. Yen, J.J. McKetta, Solubility of nitrous oxide in some nonpolar solvents, J. Chem. Eng. Data 7 (1962) 288.

[32] J.L. Herde, J.C. Lambert, C.V. Senoff, Inorganic synthesis, in: G.W. Parshall (Ed.), Inorganic Synthesis, John Wiley & Sons Inc., Hoboken, NJ, USA, 1974, pp. 18–20.

[33] S.H. Chanteau, J.M. Tour, Synthesis of anthropomorphic molecules: the NanoPutians, J. Org. Chem. 68 (2003) 8750.

[34] N.A. Yakelis, R.G. Bergman, Sodium Tetrakis[(3,5-trifluoromethyl)phenyl] borate (NaBArF(24)): safe preparation,standardized purification, and analysis of hydration, Organometallics 24 (2005) 3579.